ACTA ASTRONOMICA
Vol. **56** (2006) pp. 253–265

Period Changes of Contact Binaries in OGLE Database*

by

M. Kubiak, A. Udalski and M.K. Szymański

Warsaw University Observatory, al. Ujazdowskie 4, 00-478 Warsaw, Poland
e-mail: (mk,udalski,msz)@astrouw.edu.pl

Received July 20, 2006

ABSTRACT

Presented are results of determination of secular period changes for 569 contact binaries from the OGLE database with periods shorter than about one day and observations spanning 14 observing seasons. The statistically significant rates of secular changes found for 134 stars are distributed nearly symmetrically around zero with a half-width of the distribution equal to about $3.5\cdot10^{-7}$ day/year. The remaining rates are confined within the error distribution with dispersion about $2.3\cdot10^{-7}$ day/year. The largest rates of period change that have been found are of the order of $5\cdot10^{-6}$ day/year.

Key words: *binaries: close – binaries: eclipsing*

1. Introduction

OGLE project, devoted originally to the search for the microlensing events (Udalski, Kubiak and Szymański 1994, Udalski 2003), started in 1992 and has since that time collected a vast database of photometric observations of stars in selected directions toward the Galactic center. Although during different phases of the project different fields were observed, for some of them, namely those lying in the direction of the Baade's Window, observations since the beginning of the project exist.

These observations form a rich and uniform base for studies of different kinds of variable stars in a broad range of periods. In particular, a catalog of 2741 close binaries, identified in the first phase of OGLE project, was published by Szymański, Kubiak and Udalski (2001). It was based on four seasons of observations between 1992 and 1995. More than 1200 of these objects could be also identified in later observational seasons. About five thousand days long total time-span of observations enables a search for their secular period changes.

*Based on observations obtained with the 1.3 m Warsaw telescope at the Las Campanas Observatory of the Carnegie Institution of Washington.

Studies of the long time variations of the orbital period of contact binary stars may help to resolve the problem of their structure and evolution, in particular – the evolution of their angular momentum. A recent review of the present state of relevant theories was given *e.g.*, by Stępień (2006). Useful new observations and compilation of former results are given by Qian (2001a,b).

2. Observations

Photometric data were taken from the new OGLE databases obtained for all past seasons with the image subtraction method (Udalski 2003, Szymański 2005). Selected were objects with more than about 500 observations distributed more or less uniformly between 1992 and 2005, having periods shorter than about one day and well defined mean light curves. Finally, 682 objects were used in further analysis, although not for all of them the meaningful results could be obtained, mainly due to large observational errors and/or variability of the mean light curves. Observations for particular stars, extracted from the OGLE database, are accessible from Acta Astronomica Archive (see cover page for details) directory */acta/2006/kub_253*, as text files named with symbols: *field.number*, where *field* denotes the name of the OGLE-I field and *number* is the star number in OGLE-I database. Each file gives Heliocentric Julian Day *minus* 2 448 000 and *I*-band brightness *minus* mean from all observations of the star. All these objects are listed in Table 1, giving: name of the star; mean brightness of all observations I; observed color index $V-I$; and equatorial coordinates. Here only first entries of Table 1 are given, the entire Table 1 is available at the following URL:

ftp://ftp.astrouw.edu.pl/acta/2006/kub_253

3. Secular Period Variations

A typical OGLE field was observed every 1–5 days during each observing season. This frequency of observations is sufficient for periodogram analysis but excludes the use of the traditional $O-C$ diagram method of determining the long-term period variation from the actually observed moments of brightness minima or maxima. In the present case, when observations are separated by more than the length of the period of brightness variations, the following methods were applied.

3.1. Minimization of Variance

As a first step, all observations are Fourier- analyzed to provide a starting value of a constant period. The total length of observations guarantees the accuracy of the period determination of the order of 10^{-5} day. This starting value of the period is used to create the preliminary mean light curve and to reject all the points deviating from that mean by more than 3σ. Initial period is then varied in the limits $\pm 4\cdot 10^{-4}P$ by steps of $10^{-7}P$. For each trial value of period the observations are

T a b l e 1

Contact binaries in OGLE database used for determination of secular period changes. Given are: name of the object, period in days, observed brightness in band I, observed color index $V-I$ ("9.99" means lack of data) and equatorial coordinates.

Star		P [day]	I	$V-I$	α_{2000}	δ_{2000}
bw4	17835	0.227737	15.93	1.51	$18^h03^m46\overset{s}{.}00$	$-29°47'40\overset{''}{.}1$
bw5	166779	0.239191	18.48	9.99	$18^h02^m35\overset{s}{.}99$	$-29°55'37\overset{''}{.}1$
bw1	86175	0.248869	16.48	1.27	$18^h02^m18\overset{s}{.}58$	$-29°56'23\overset{''}{.}5$
bw9	241162	0.251756	16.81	1.81	$18^h01^m12\overset{s}{.}75$	$-29°51'28\overset{''}{.}7$
bw4	22394	0.258262	15.71	1.19	$18^h03^m47\overset{s}{.}69$	$-29°44'44\overset{''}{.}8$
bw3	168639	0.259800	18.15	1.67	$18^h04^m45\overset{s}{.}11$	$-30°11'40\overset{''}{.}5$
bw6	148962	0.260140	18.72	1.74	$18^h03^m31\overset{s}{.}78$	$-30°13'21\overset{''}{.}2$
bw4	114518	0.264038	18.17	1.61	$18^h04^m21\overset{s}{.}03$	$-29°48'42\overset{''}{.}5$
bw2	69778	0.266274	19.03	9.99	$18^h02^m10\overset{s}{.}01$	$-30°19'25\overset{''}{.}8$
bw1	174918	0.269860	18.98	9.99	$18^h02^m37\overset{s}{.}68$	$-29°43'44\overset{''}{.}8$
bw9	251588	0.270142	17.36	1.42	$18^h01^m16\overset{s}{.}16$	$-29°47'12\overset{''}{.}5$
bw4	112207	0.270313	19.26	1.43	$18^h04^m15\overset{s}{.}39$	$-29°50'50\overset{''}{.}1$
bw6	64393	0.270455	18.04	1.55	$18^h03^m11\overset{s}{.}35$	$-30°20'57\overset{''}{.}2$
bwc	111858	0.271142	18.59	1.34	$18^h03^m20\overset{s}{.}17$	$-30°05'24\overset{''}{.}7$
bw6	139978	0.273040	19.07	1.93	$18^h03^m29\overset{s}{.}76$	$-30°17'19\overset{''}{.}2$
bw5	177625	0.273625	17.16	1.40	$18^h02^m49\overset{s}{.}26$	$-30°03'11\overset{''}{.}8$
bw4	178	0.278349	16.54	1.26	$18^h03^m54\overset{s}{.}77$	$-29°56'55\overset{''}{.}9$
bwc	132962	0.279882	19.18	2.24	$18^h03^m14\overset{s}{.}24$	$-29°58'26\overset{''}{.}4$
bwc	28265	0.282410	18.20	9.99	$18^h02^m46\overset{s}{.}11$	$-29°56'28\overset{''}{.}9$
bw1	15384	0.283391	16.00	1.21	$18^h01^m45\overset{s}{.}80$	$-29°47'11\overset{''}{.}9$
bw6	152319	0.286912	16.05	1.43	$18^h03^m30\overset{s}{.}16$	$-30°10'38\overset{''}{.}2$
bw8	24569	0.287683	17.78	1.50	$18^h02^m51\overset{s}{.}61$	$-29°44'28\overset{''}{.}9$
bw3	155221	0.288895	17.41	1.76	$18^h04^m48\overset{s}{.}25$	$-30°18'10\overset{''}{.}8$
bw5	90502	0.290357	17.93	1.60	$18^h02^m23\overset{s}{.}96$	$-30°04'40\overset{''}{.}1$
bw2	135582	0.291086	17.67	1.47	$18^h02^m28\overset{s}{.}20$	$-30°20'25\overset{''}{.}8$
bw8	199379	0.291343	18.46	1.43	$18^h03^m37\overset{s}{.}68$	$-29°42'28\overset{''}{.}8$
bw6	2078	0.294554	18.64	1.47	$18^h02^m52\overset{s}{.}69$	$-30°21'22\overset{''}{.}0$
bw4	142014	0.296267	16.82	1.30	$18^h04^m29\overset{s}{.}67$	$-29°51'46\overset{''}{.}8$
bw3	3282	0.296737	15.73	1.16	$18^h03^m52\overset{s}{.}33$	$-30°20'28\overset{''}{.}8$
bwc	1362	0.296936	18.74	1.30	$18^h02^m51\overset{s}{.}58$	$-30°09'19\overset{''}{.}9$
bw4	41816	0.297685	17.56	1.46	$18^h03^m55\overset{s}{.}19$	$-29°51'56\overset{''}{.}5$
bw4	131051	0.300945	19.18	9.99	$18^h04^m20\overset{s}{.}21$	$-29°42'51\overset{''}{.}6$
bwc	249888	0.301219	15.97	1.20	$18^h03^m42\overset{s}{.}83$	$-29°54'24\overset{''}{.}1$
bw2	20210	0.302603	19.25	9.99	$18^h01^m50\overset{s}{.}69$	$-30°14'25\overset{''}{.}5$
bw2	107002	0.303322	17.86	1.48	$18^h02^m23\overset{s}{.}84$	$-30°17'58\overset{''}{.}7$

grouped in 25 phase bins, average brightness in each bin is determined, squared deviation of observations from the mean in each bin is calculated, and finally, the variance is determined as

$$\mathrm{Var}(P,0) = \frac{1}{N-26}\sum_{k=1}^{25}\sum_{i=1}^{N_k}(\overline{I_k} - I_i)^2$$

where N_k is a number of observations I_i falling in k-th phase-bin, $\overline{I_k}$ is a mean brightness in k-th bin, and N is a total number of observations of a given star. Period value P_0, for which the variance attains a minimum, is adopted as the "best" constant-period value.

This procedure of variance calculations is repeated for a grid of pairs $(P, \mathrm{d}P/\mathrm{d}t)$ where period P (in days) is varied in the same limits as above and the time derivative of frequency, $\mathrm{d}\omega/\mathrm{d}t = -(2\pi/P^2)\mathrm{d}P/\mathrm{d}t$, is varied in the range $\pm 4\cdot 10^{-7}$ rad/day^2 in steps of 10^{-9} rad/day^2. The minimum value of variance $\mathrm{Var}(P_1, \mathrm{d}P/\mathrm{d}t)$ determines the period P_1 and its time derivative best fitting the observations at the hypothesis of secular period changes. This value of variance could be directly compared with minimum value of $\mathrm{Var}(P_0,0)$ obtained at the hypothesis of constant period.

In the present calculations two-parameter fit gave always lower or the same value of variance than the one-parameter fit. To estimate the probability that this difference is real we used the ratio-of-variances method as described by Lampton, Margon and Bowyer (1976), calculating for each star the statistic

$$\mathcal{F} = \frac{\mathrm{Var}(P_0,0)}{\mathrm{Var}(P_1, \mathrm{d}P/\mathrm{d}t)}.$$

The difference between the hypothesis of constant period and hypothesis of variable period is real if

$$\mathcal{P} \equiv (\mathcal{F} - 1) \times (N - 27) > F(1, N, 0.1)$$

where $F(1,N,0.1)$ is the Fisher-Snedecor distribution for degrees of freedom 1 and N at the significance level 0.1. From the tables of this distribution it follows that for $N > 400$ the value of F practically does not depend on N and is equal to 63.3. Period changes of the objects having $\mathcal{P}$-statistic greater than 63.3 can be considered as statistically confirmed.

The results are collected in Table 2 where the consecutive columns give: symbol of the star, the "best" value of period, period derivative in day/year, number of observations and values of $\mathcal{F}$ and $\mathcal{P}$-statistics. Full Table 2 containing data for 569 stars is provided in Acta Astronomica Archive account given above. Here we reproduce only its sample page.

A few examples, illustrating the effect the allowance for the period secular change has on the phased light curve, are given in Fig. 1. For each star the upper

T a b l e 2

Time derivatives of periods determined by the method of variance minimization. Columns give: name of the object, period in days, rate of period change in day/year, number of observations, statistics $\mathcal{F}$ and $\mathcal{P}$.

Star		P_1 [day]	dP/dt [day/year]	N	$\mathcal{F}$	$\mathcal{P}$
bw5	166779	0.2391916	0.19E – 06	878	1.073	64.0
bw1	86175	0.2488694	0.40E – 07	1193	1.013	15.5
bw9	241162	0.2517571	−0.18E – 06	753	1.041	30.8
bw6	157469	0.2581246	0.17E – 06	733	1.168	123.0
bw4	22394	0.2582609	0.43E – 07	907	1.014	12.7
bw3	168639	0.2598006	0.20E – 06	800	1.123	98.3
bw6	148962	0.2601409	−0.13E – 06	685	1.070	47.9
bw4	114518	0.2640387	−0.10E – 06	783	1.051	39.9
bw2	69778	0.2662757	−0.21E – 06	796	1.017	13.5
bw1	174918	0.2698598	0.18E – 06	917	1.067	61.4
bw9	251588	0.2701431	0.18E – 06	744	1.347	257.8
bw4	112207	0.2703129	0.21E – 07	776	1.018	14.0
bw6	64393	0.2704557	−0.17E – 06	732	1.021	15.4
bwc	111858	0.2711405	−0.64E – 07	780	1.024	18.7
bw6	139978	0.2730297	−0.19E – 06	729	1.023	16.7
bw5	177625	0.2736237	0.21E – 06	1171	1.252	294.8
bwc	132962	0.2798811	0.32E – 07	789	1.027	21.3
bwc	28265	0.2824107	−0.79E – 07	1154	1.013	15.0
bw1	15384	0.2833913	−0.11E – 06	833	1.022	18.3
bw6	152319	0.2869125	0.16E – 06	760	1.436	330.9
bw3	155221	0.2888988	−0.74E – 06	797	2.145	911.4
bw2	135582	0.2910865	0.19E – 06	804	1.161	129.3
bw8	199379	0.2913430	0.22E – 06	613	1.029	17.7
bw4	142014	0.2962651	0.66E – 07	723	1.053	38.3
bw3	3282	0.2967375	0.20E – 07	1023	1.101	103.2
bwc	1362	0.2969302	0.97E – 06	948	1.180	170.5
bw8	169332	0.3012195	−0.61E – 06	720	1.926	665.8
bwc	249888	0.3012192	−0.55E – 06	935	1.719	671.5
bw2	20210	0.3026027	0.53E – 08	799	1.016	12.8
bw2	36193	0.3026951	−0.10E – 06	803	1.033	26.5
bw7	106862	0.3040424	0.16E – 06	951	1.040	38.0
bw3	30401	0.3055694	−0.11E – 05	805	1.212	170.4
bwc	127313	0.3061566	−0.24E – 06	805	1.055	44.2
bw5	173703	0.3063743	0.11E – 05	602	1.087	52.3
bwc	229688	0.3071223	0.99E – 07	1032	1.009	9.3
bw3	6690	0.3071931	−0.17E – 06	1006	1.086	86.4
bw5	114525	0.3074514	−0.33E – 07	880	1.020	17.6

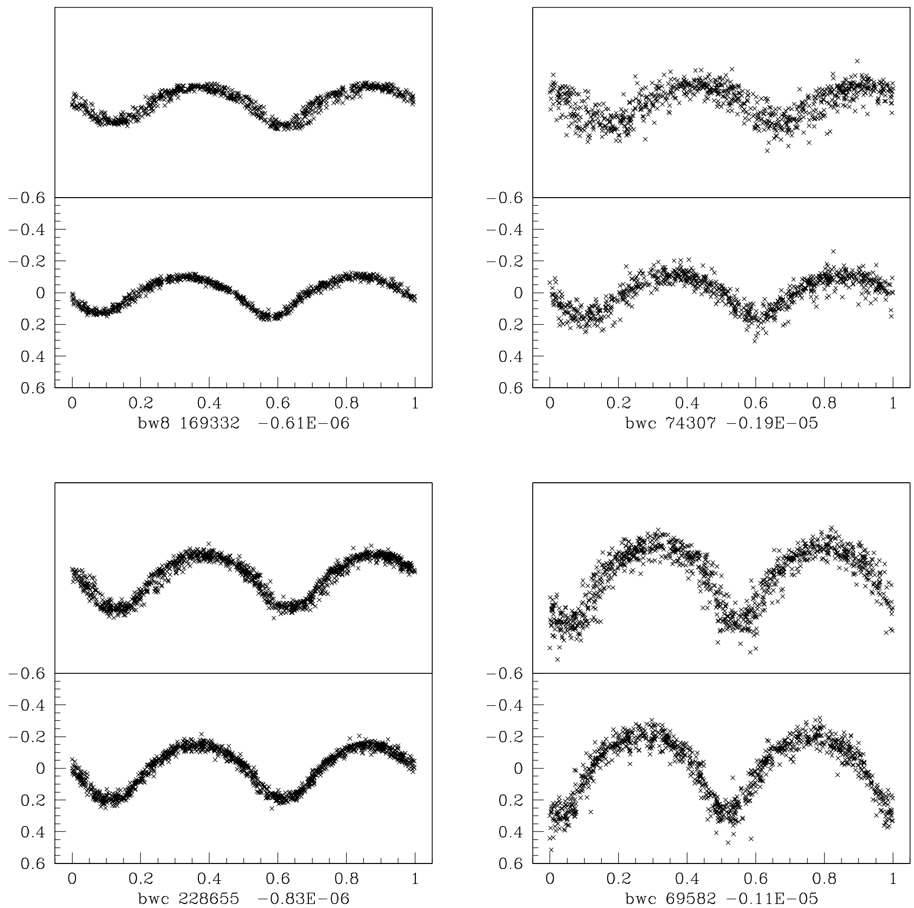

Fig. 1. Examples of the mean light curves phased with the best constant period (*upper panels*) and the period changing at a rate (in day/year) given for each object (*lower panels*).

panel shows the result of phasing with the best value of constant period and lower panel shows the result of phasing when the secular period variation (its value is given in Fig. 1) is taken into account. The diminishing of the scatter of observational points around the phased light curve is clearly visible.

To check for the possible presence of systematic errors and also to assess a realistic estimate of the probable errors of obtained secular period changes we used also the following independent method.

3.2. "Average $O-C$ Diagrams"

Although our data are distributed too sparsely to allow the use of the classic $O-C$ method we tried to modify it by finding the "temporary" light curves in different segments of the total observing period.

We made the assumption that the true light curves of our contact binaries can be approximated by a sum of four harmonics:

$$I(t) = \sum_{i=1}^{4}\left(a(i)\cos\left(\frac{2\pi}{P}t\right) + b(i)\sin\left(\frac{2\pi}{P}t\right)\right).$$

As a first step we determined the parameters $a(i)$ and $b(i)$ by standard least-square method from all observational points, using the value of period P found from the periodogram analysis and corrected by minimizing the scatter of points around the mean light curve, similarly as in the method described above. Practice shows that adding more harmonics or changing slightly the assumed period does not affect markedly the resulting "overall" mean light curve.

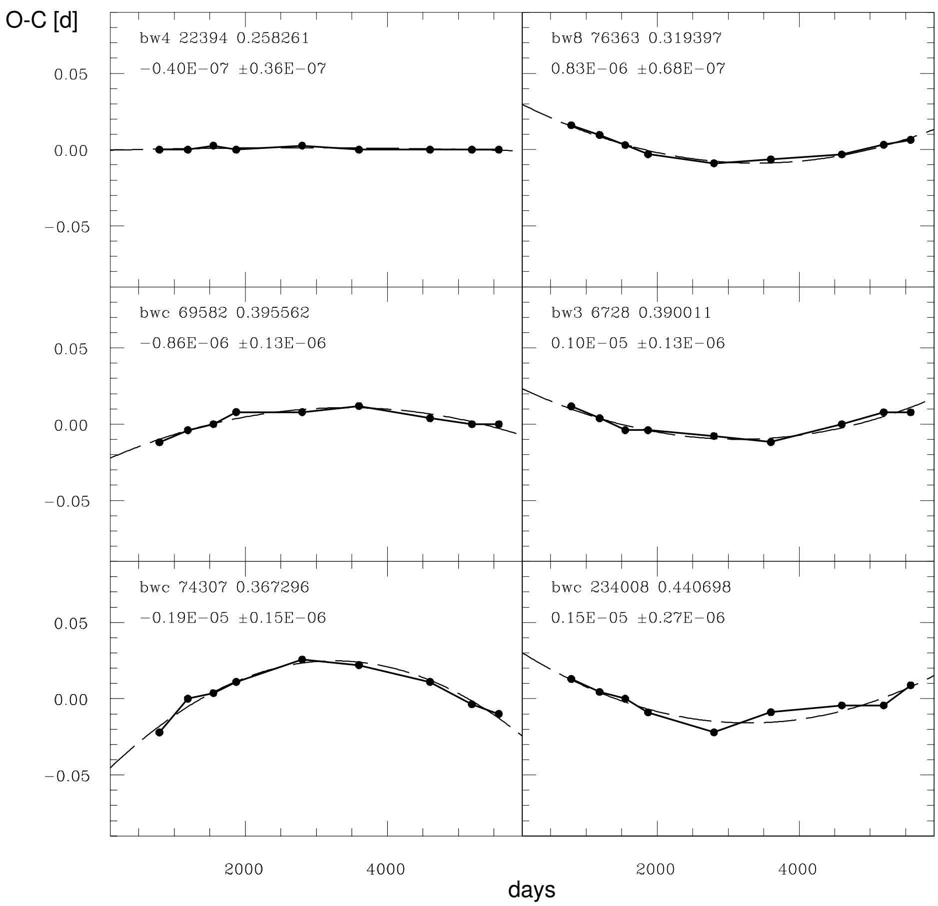

Fig. 2. Examples of "average $O-C$ diagrams" obtained by the method described in text. In each panel given are: symbol of the star, adopted period in days, rate of secular period change and its error, both in day/year.

Then, the entire period of observations was divided into 9 segments containing more or less the same number of observational points. The parameters $a(i)$ and $b(i)$ were calculated from the data in each segment providing nine "temporary" light curves.

The difference between the moments of minima of the "overall" mean light curve and the "temporary" light curve in a given time segment was treated as the $O-C$ value in this segment. The moments of time located approximately at the middle of each segment represented the "epochs" of the segments. These "epochs" were the same for all stars and equal to JD 2448000 + 790, 1190, 1550, 1870, 2800, 3600, 4600, 5190, and 5570. With these data the "average $O-C$ diagram" was constructed and its quadratic term, *i.e.*, secular period change, was determined. A few examples of typical "average $O-C$ diagrams" are shown in Fig. 2. The results for 272 stars, for which the described procedure gave acceptable "average" $O-C$ diagrams are given in Table 3. The respective columns of Table 3 give symbol of the star, adopted period P, secular change of period in day/year resulting from the quadratic term and its formal error.

4. Errors

We feel that the method of variance minimization, which does not depend on any assumptions about the shape of the light curve, should give the most reliable results. On the other hand, although the $\mathcal{F}$-statistics in this case is a good measure of the statistical significance of obtained results, the error estimation is not directly given. We think, however, that a good estimation of the real errors can be obtained by comparing the results obtained by both methods described above. This is done in graphic form in upper part of Fig. 3. The distribution of the scatter of points around the broken line is shown in lower part of Fig. 3. The broken line in Fig. 3 is a Gaussian fitted to the shown histogram. Although the fit is rather poor in the wings, we think that the dispersion of the Gaussian, equal to $2.3 \cdot 10^{-7} (\pm 0.20 \cdot 10^{-7})$, can be accepted as a realistic measure of the error with which the rate of secular period change could be determined from the present data.

It may be also interesting to compare the period changes obtained by both methods described above for 60 objects with $\mathcal{P}$-statistic greater than 63.3. It is done in upper panel of Fig. 4. The distribution of markedly smaller differences, shown in lower panel of Fig. 4, has a characteristic width of $1.11 \cdot 10^{-7}$ day/year. This suggests very strongly that the error of both methods is in reality smaller than the error accepted above, and that the distribution of error in Fig. 3 contains also a contribution from the true scatter of period change rates smaller than $2.3 \cdot 10^{-7}$ day/year.

Table 3

Results of the "average $O-C$ diagram" method. Table gives: name of the object, adopted period P in days, number of observations, rate of the period change in day/year determined from the quadratic term in the $O-C$ diagram and formal error of the solution.

Star		P [day]	N	$\mathrm{d}P/\mathrm{d}t$ [day/year]	p.e.
bw5	166779	0.239193	878	0.16E − 06	0.92E − 07
bw1	86175	0.248869	1193	−0.63E − 07	0.16E − 06
bw9	241162	0.251756	753	−0.19E − 06	0.28E − 06
bw6	157469	0.258126	733	0.10E − 06	0.75E − 07
bw4	22394	0.258261	907	−0.41E − 07	0.37E − 07
bw3	168639	0.259802	800	0.10E − 06	0.62E − 07
bw6	148962	0.260140	685	0.20E − 08	0.67E − 07
bw4	114518	0.264038	783	−0.42E − 08	0.87E − 07
bw2	69778	0.266274	796	−0.20E − 06	0.96E − 07
bw1	174918	0.269861	917	0.10E − 06	0.32E − 07
bw9	251588	0.270144	744	0.21E − 06	0.74E − 07
bw6	64393	0.270454	732	−0.13E − 06	0.19E − 06
bwc	111858	0.271140	780	−0.19E − 06	0.18E − 06
bw6	139978	0.273028	729	−0.68E − 07	0.12E − 06
bw5	177625	0.273625	1171	0.11E − 06	0.52E − 07
bwc	28265	0.282410	1154	0.14E − 06	0.32E − 07
bw1	15384	0.283391	833	−0.29E − 06	0.10E − 06
bw6	152319	0.286914	760	0.23E − 06	0.65E − 07
bw3	155221	0.288894	797	−0.89E − 06	0.77E − 07
bw2	135582	0.291088	804	0.97E − 07	0.50E − 07
bw4	142014	0.296266	723	−0.13E − 06	0.23E − 06
bw8	169332	0.301215	720	−0.34E − 06	0.19E − 06
bwc	249888	0.301216	935	−0.34E − 06	0.16E − 06
bw2	36193	0.302694	803	0.14E − 07	0.18E − 06
bw7	106862	0.304043	951	0.76E − 07	0.16E − 06
bwc	127313	0.306155	805	−0.21E − 08	0.12E − 06
bwc	229688	0.307123	1032	0.37E − 06	0.24E − 06
bw3	6690	0.307192	1006	−0.21E − 06	0.65E − 07
bw5	114525	0.307451	880	−0.20E − 06	0.11E − 06
bw3	39597	0.311137	756	0.34E − 06	0.54E − 07
bw2	196028	0.313653	1084	0.30E − 07	0.10E − 06
bw1	40225	0.313943	871	0.24E − 06	0.61E − 07
bw3	96021	0.314053	809	−0.55E − 06	0.16E − 06
bw1	99167	0.314362	883	0.23E − 06	0.16E − 06
bw6	124970	0.317218	811	−0.77E − 07	0.16E − 06

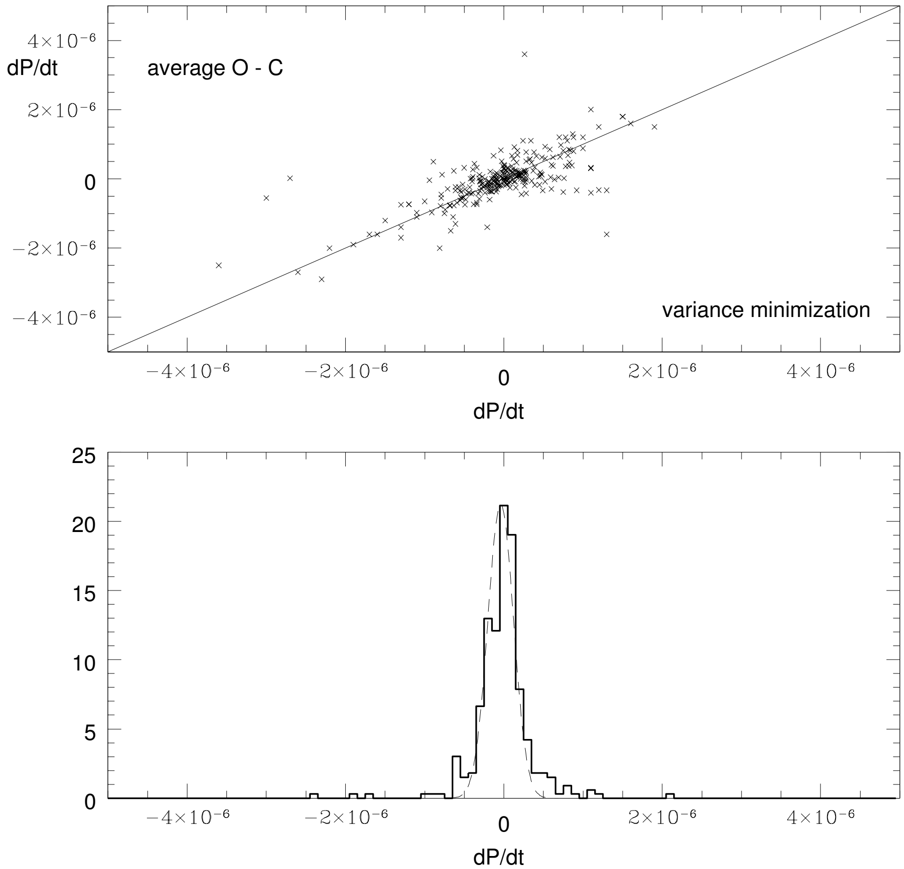

Fig. 3. *Upper panel:* comparison of secular period changes obtained by minimization of variance and "average $O-C$ diagrams" methods. *Lower panel:* distribution of deviations from the broken line, adopted as a representation of the error distribution.

5. Results

Histograms drawn with thick continuous lines in Fig. 5 summarize the results obtained in this work and presented in Table 2. All the histograms are normalized to total number of objects equal to 100. The top panel shows the distribution of $\mathrm{d}P/\mathrm{d}t$ values obtained for 134 stars for which $\mathcal{P}$ is bigger than 63.3, *i.e.*, the objects for which period changes are determined most reliably. It clearly proves that contact binaries show the same tendency both to lengthen and to shorten their periods. Our total span of observations is too short to decide if this is a consequence of periodic period changes in rather short time scale of the order of dozens of years, or it is a secular variation in longer time scale.

In the same panel the histogram marked with dotted line shows the distribution of secular period changes of 42 objects determined in previous works and taken

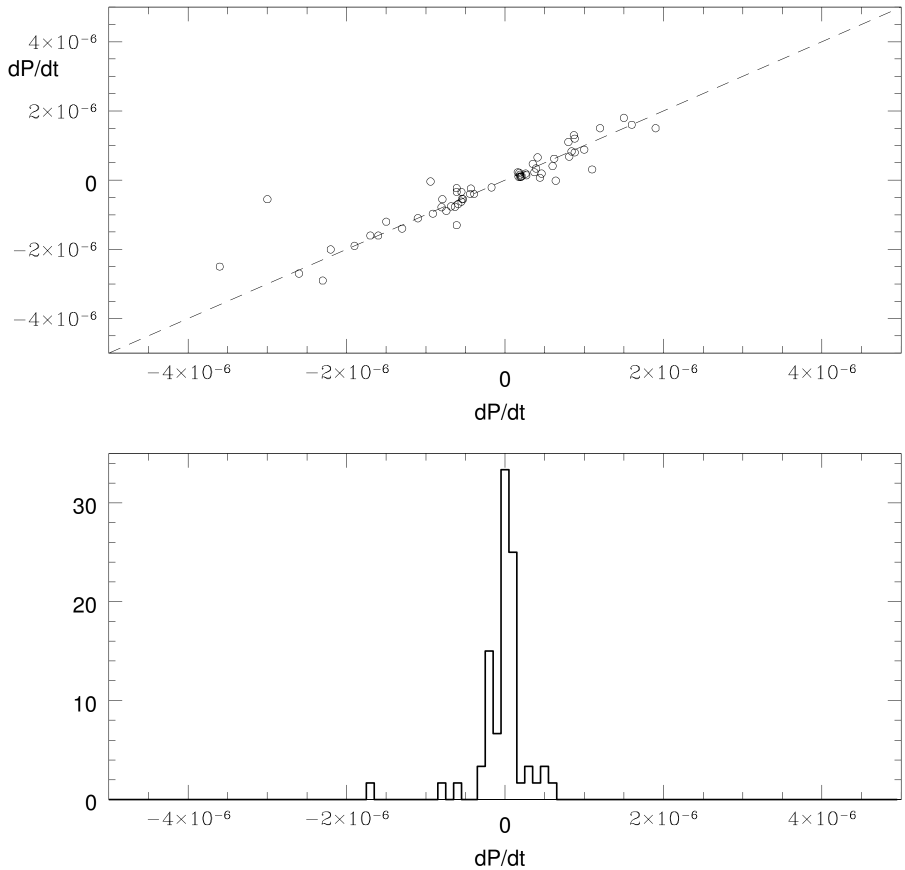

Fig. 4. The same as in Fig. 3 but for objects with $\mathcal{P} > 63.3$.

from the compilation by Qian (2001a,b). Dealing with photometric observations only, we are not able to distinguish W and A type contact binaries and draw any conclusions regarding the possible difference in period variations of both groups. Nevertheless, the former determinations seem to be in general agreement with the present results: The majority of contact systems change their periods with time scale not exceeding $1 \cdot 10^{-6}$ day/year. The rates larger than about $5 \cdot 10^{-6}$ day/year seem to be very rare and were not observed.

The top histogram in Fig. 5 shows a marked deficit of objects at small (smaller than the adopted error) but statistically significant period changes. This is an obvious result of the fact that for the objects with very small period changes the $\mathcal{F}$-statistics should be close to one from definition and the statistically meaningful confirmation of these changes would need correspondingly bigger number and/or better accuracy of observations. These objects in natural way populate the central part of diagrams shown in both lower panels of Fig. 5 and fill up the central part of the dotted histogram.

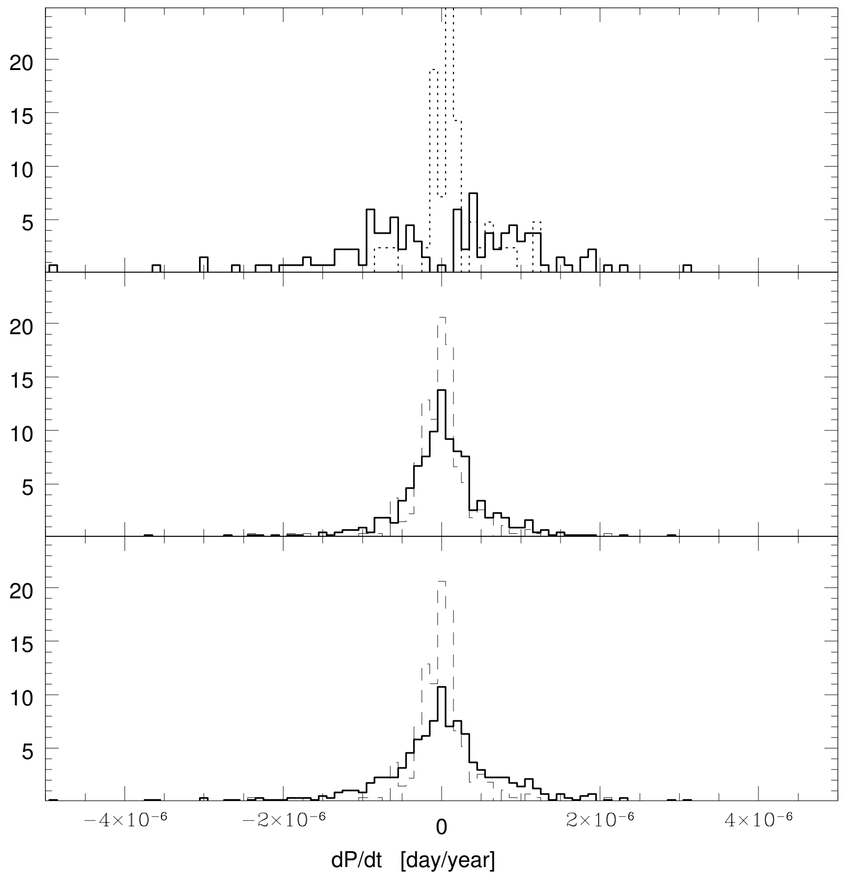

Fig. 5. *Top panel:* distribution of period changes of the objects with $\mathcal{P}$>63.3. Dotted histogram shows the distribution of period changes determined in previous works. *Middle panel:* distribution of period changes for the objects for which $\mathcal{P}$< 63.3. *Lower panel:* distribution of period changes of all objects in our sample. Broken line histograms mark the error distribution from Fig. 3.

Middle panel of Fig. 5 shows the distribution of objects for which $\mathcal{P}$ is smaller than 63.3 and the lower panel shows the distribution of all 569 objects in our sample. The error distribution from Fig. 3 is repeated with broken line. Simple χ^2 test confirms the close resemblance of all these histograms.

Summing up we may conclude, that the majority of contact systems analyzed in our sample of stars in the direction of the Baade's Window changes their periods at the rates not exceeding about $\pm 2.3 \cdot 10^{-7}$ day/year. Only 123 objects have statistically confirmed greater rates and no object with the rate greater than $5 \cdot 10^{-6}$ day/year was found. There is also no obvious correlation between the period change rate and other characteristics, such as I-brightness, $V-I$ color or period length, except for a slight suggestion that the systems with the shortest periods (0.2–0.3 day) all have secular period changes very close to zero.

Acknowledgements. We are indebted to Professor Andrzej Kruszewski for his expert comments on the statistical part of this work. This work was partly supported from the MNiSW DST grant to the Warsaw University Observatory.

REFERENCES

Lampton, M., Margon, B., and Bowyer, S. 1976, *Astrophys. J.*, **208**, 177.
Press, W.H., Teukolsky, S.A., Vetterlink, W.T., and Flannery, B.P. 1996, "Numerical Recipes in Fortran 77", Cambridge University Press.
Qian, S. 2001a, *MNRAS*, **328**, 635.
Qian, S. 2001b, *MNRAS*, **328**, 914.
Stępień, K. 2006, *Acta Astron.*, **56**, 199.
Szymański, M.K. 2005, *Acta Astron.*, **55**, 43.
Szymański, M., Kubiak, M. and Udalski, A. 2001, *Acta Astron.*, **51**, 259.
Udalski, A. 2003, *Acta Astron.*, **53**, 291.
Udalski, A., Kubiak, and M., Szymański, M. 1994, *Acta Astron.*, **44**, 319.